PHYSICSAccess Research Paper
ISSN Online: 2756-3898, ISSN Print: 2714-500X https://doi.org/10.47514/phyaccess.2025.5.1.002

Profiling the Properties of SILAR Synthesized MnSe Films as Potential Material for Absorber Layer of Thin Film Solar Cells

Asielue O Kingsley[1], Opene J Nkechi[1] and Okoli N Livinus[2]

[1] Department of Science Laboratory Technology, Delta State Polytechnic, Ogwashi-Uku, Delta State Nigeria
[2] Department of Computer Science Education, Madonna University Nigeria, Okija Campus, Anambra State, Nigeria

Corresponding E-mail: kingslaw2016@yahoo.com

Received 22-12-2024
Accepted for publication 27-01-2025
Published 28-01-2025

Abstract

This study investigates the optical, structural, and electrical properties of manganese selenide (MnSe) thin films synthesized using the Successive Ionic Layer Adsorption and Reaction (SILAR) method, with varying volumes of triethylamine (TEA) as a complexing agent. The MnSe films exhibited high absorbance in the ultraviolet (UV) region, peaking at values from 0.61 to 0.91 depending on TEA concentration, and declining towards the near-infrared (NIR) region. Transmittance varied from 12.53% to 92.17%, decreasing with higher TEA concentrations. The energy band gap of the films decreased from 2.90 eV with 2 ml of TEA to 2.30 eV with 10 ml, highlighting the tunability of MnSe for photovoltaic applications. Film thickness varied from 190.82 nm to 381.63 nm, reflecting a direct relationship with TEA concentration. Structurally, the MnSe films crystallized in the cubic phase with improved crystallinity and reduced defects at higher TEA volumes, as evidenced by a crystallite size increase from 20.10 nm to 25.09 nm and decreased dislocation density and microstrain. Morphological analysis revealed uniform grain-like structures at moderate TEA concentrations, which are optimal for photovoltaic performance. The electrical properties highlighted a trade-off between resistivity and conductivity. Films deposited with lower TEA volumes exhibited higher electrical conductivity of 2.72×10^{-5} S/cm at 2 ml compared to 1.02×10^{-5} S/cm at 10 ml. These findings confirm the suitability of MnSe thin films for absorber layers in solar cells, particularly where tunable optical and electrical properties are desired. The ability to control these properties by varying TEA concentration enhances the material's versatility for applications beyond photovoltaics, including optoelectronic and photodetector devices.

Keywords: SILAR; MnSe; Nanofilms; Solar cell; Absorber layer.

I. INTRODUCTION

The increasing need for clean and renewable energy has led to extensive research in the development of thin-film solar cells. One of the critical components in these cells is the absorber layer, which determines the device's ability to convert sunlight into electricity. Transition metal chalcogenides have been explored as promising materials for

this purpose due to their tunable optical and electronic properties. Manganese selenide (MnSe), a manganese chalcogenide, has garnered attention due to its potential as an absorber material in thin film solar cells owing to its excellent optical and semiconducting properties [1], [2]. Manganese selenide exists in multiple crystal phases, including cubic (rock-salt), hexagonal (wurtzite), and zinc blend structures. The cubic structure is the most thermodynamically stable form of MnSe, whereas the wurtzite phase is metastable and often associated with enhanced magnetic and optical properties [3], [4]. These properties arise from the sp-d exchange interactions between the 3d electrons of Mn^{2+} and the conduction band states [5], [6]. These interactions, along with the ability to control MnSe's phase and morphology during synthesis, make it an attractive candidate for photovoltaic applications [6], [7].

Various methods have been explored for the synthesis of MnSe thin films, including hydrothermal synthesis [6-7], e-beam evaporation [8], reactive pulsed laser deposition [9], molecular beam epitaxy [10], electrodeposition [11], vapor–liquid–solid growth technique [12], colloidal approach [13], chemical bath method [14] and others. While these methods have been successful in producing high-quality MnSe films, they often require complex setups and high temperatures, which limit their scalability [7], [9]. The Successive Ionic Layer Adsorption and Reaction (SILAR) technique provides a cost-effective alternative that allows for precise control over film thickness and uniformity [15-17]. Among the cost-effective thin film deposition methods, the SILAR process has enabled the growth of binary thin films such as Cu_3Se_2, Sb_2Se_3, and CdSe at relatively low temperatures, making it suitable for large-scale solar cell fabrication [18]. Many binary chalcogenide thin films such as CoSe [19-20], CuSe [21-22], ZnSe [23-24], Dy2Se3 [25], InSe [26], CdSe [27] and CdSe/ZnSe [28] have been synthesized using SILAR approach.

MnSe also exhibits unique magnetic properties, particularly in the wurtzite phase, where it demonstrates low-temperature spin-glass behaviour due to its non-compensated surface spins [29]. This unique characteristic arises from the structural and electronic properties of the material, which have been explored through various synthesis methods and theoretical analyses. These properties make MnSe an exciting material not only for photovoltaic applications but also for spintronic devices [10, 30]. The ability to tune the properties of MnSe thin film through variation of growth parameters further enhances its suitability as a versatile material for energy-related applications.

This study focuses on synthesizing manganese selenide (MnSe) thin films using the SILAR method and investigating their structural, optical, electrical, compositional, and morphological properties with varying concentrations of triethanolamine (TEA). The key contribution lies in demonstrating how TEA concentrations systematically modulate these properties, enabling tailored optimization for photovoltaic applications while evaluating MnSe's potential as an absorber layer in thin-film solar cells. Additionally, this work highlights the practical scalability of the SILAR method for cost-effective and precise thin-film fabrication, contributing to ongoing research aimed at achieving high efficiency in photovoltaic devices.

II. EXPERIMENTATION

Manganese selenide (MnSe) thin films were fabricated using the Successive Ionic Layer Adsorption and Reaction (SILAR) method. The reagents used included manganese (II) chloride tetrahydrate ($MnCl_2{\cdot}4H_2O$), selenium powder, sodium sulphite and distilled water. A 100 mM solution of manganese (II) chloride tetrahydrate was prepared by dissolving 9.90 g of $MnCl_2{\cdot}4H_2O$ in 500 ml of distilled water. The newly prepared 100 mM of sodium selenosulphite (Na_2SeSO_3) at pH~11.2 was obtained by refluxing according to the processes given by [31]. Similar success of selenium had been used by [32-37] for the deposition of binary metal selenide thin films. Reference [18] had recently opined the use of Na_2SeSO_3 as a source of selenium in thin film deposition by the SILAR method. The chemical equation for the formation of $NaSeSO_3$ is given by (1).

$$Se_{(s)} + Na_2SO_{3_{(aq)}} \xrightarrow{90\,^{\circ}\mathrm{C}\,(3\,hours)} NaSeSO_{3_{aq}} \qquad (1)$$

This freshly prepared colourless $NaSeSO_3$ solution was used immediately due to its instability. Triethanolamine (TEA), a complexing agent with a molar mass of 149.19 g/mol, was used in varying volumes (2 ml, 4 ml, 6 ml, 8 ml, and 10 ml) to complex the manganese precursor. 1M of ammonium solution was used to provide OH^- ions that made up the reacting species for the deposition of MnSe thin films. The dissociation of these reactants in an aqueous solution is described below.

1) Sodium selenosulfate ($NaSeSO_3$) dissociates as follows:

$$NaSeSO_{3_{(aq)}} \rightarrow Na^+_{aq} + SeSO^{2-}_3\ (aq) \qquad (2)$$

2) Manganese (II) chloride tetrahydrate ($MnCl_2{\cdot}4H_2O$) dissociates as:

$$MnCl_2 \cdot 4H_2O \rightarrow Mn^{2+}_{aq} + 2Cl^-_{aq} + 4H_2O \qquad (3)$$

3) Ammonium solution dissociates as

$$NH_3 + H_2O \rightarrow NH^+_4 + OH^- \qquad (4)$$

4) Triethylamine (TEA) acts as a base and coordinates with the manganese ion to form the manganese-TEA complex:

$$TEA_{aq} + Mn^{2+}_{aq} \rightarrow [Mn(TEA)]^{2+}_{aq} \qquad (5)$$

The deposition of MnSe thin films was carried out at room temperature, with a SILAR cycle consisting of four steps:

(i) adsorption of Mn^{2+} ions onto the substrate by immersing it in a 0.1 M manganese chloride tetrahydrate solution complexed with TEA for a dip time (t_d)of 30 seconds,
(ii) rinsing the substrate with distilled water for 10 seconds to remove loosely bound Mn^{2+} ions,
(iii) immersion in freshly prepared sodium hydrogen selenide solution for 30 seconds to allow Se^{2-} ions to react with the adsorbed Mn^{2+} ions, forming MnSe films, and

(iv) a final rinsing step with distilled water for 10 seconds to remove unreacted ions.

This process was repeated for 10 cycles to achieve uniform MnSe thin films. The total time for one SILAR (t_{SILAR}) cycle as shown in Fig. 1 was 80 seconds. Post-deposition heat treatment of films was carried out. The deposited films were annealed at 573 K for 1 hour to improve crystallinity and remove residual water molecules.

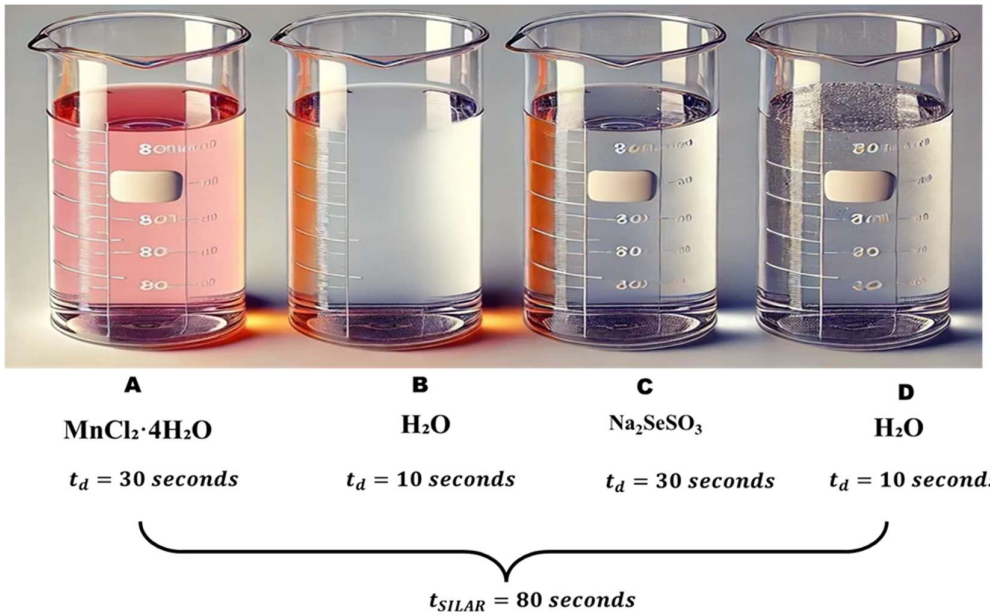

Fig. 1. Bath constituent for SILAR deposition of MnSe thin films.

The chemical equation for the formation of MnSe thin film is given by (6).

$$[Mn(TEA)]^{2+}_{aq} + SeSO^{2-}_{3\ (aq)} \rightarrow MnSe + SO^{2-}_{4} + TEA + H_2O \quad (6)$$

Fig. 1 illustrates the SILAR method used for MnSe thin film deposition. The uniqueness of the SILAR method lies in its ability to precisely control the thin film's thickness by adjusting parameters such as dipping and rinsing time, concentration of solutions, and number of cycles. Structural characterization was performed using X-ray diffraction (XRD) with an Empyrean diffractometer, and crystallite sizes were calculated using the Debye-Scherrer formula. Electrical conductivity measurements were carried out using the four-point probe technique, with resistivity and conductivity values calculated based on the film thickness determined by the gravimetric method. The experiment aimed to study the effect of varying volumes of TEA on the structural and electrical properties of the deposited MnSe thin films.

III. RESULTS AND DISCUSSION

A. Optical Properties of Manganese Selenide Thin Films

The optical properties of SILAR-deposited Manganese selenide thin films are presented in this section. The optical study was conducted within the wavelength of 300 – 1100 nm which represents the ultraviolet (UV), visible light (VIS) and near infrared (NIR) portion of the electromagnetic radiation. Optical properties studied are absorbance, transmittance, reflectance, refractive index, extinction coefficient, band gap and variation of average film thickness and energy band gap with volume concentration of TEA. Absorbance (A) values of the films were obtained with the help of a UV-VIS spectrophotometer, while other optical properties such as transmittance, reflectance, extinction coefficient, refractive index and energy band gap were calculated using (7), (8), (9), (10) and (11) respectively [38 – 41].

$$Transmittance\ (T) = 10^{-A} \quad (7)$$

$$Reflectance\ (R) = 1 - (A + T) \quad (8)$$

$$\text{Extinction coefficient (k)} = \frac{\alpha\lambda}{4\pi} \quad (9)$$

$$Refractive\ index\ (\eta) = \frac{1+R}{1-R} + \sqrt{\frac{4R}{(1-R)^2} - k^2} \quad (10)$$

$$Energy\ band\ gap = (\alpha hv)^n = \beta\left(hv - E_g\right) \quad (11)$$

Where β is a constant, $n = 2$ for direct band gap. The energy band gaps of the films were obtained by extrapolating the straight portion of the plot of $(\alpha hv)^2$ against the photon energy (hv) at $(\alpha hv)^2 = 0$

Fig. 2 illustrates the absorbance of MnSe thin films across varying wavelengths. The absorbance peaks in the UV region and declines as wavelength increases. Higher concentrations of TEA (triethanolamine) in the deposition solution lead to greater absorbance. Specifically, MnSe films deposited with increasing volumes of TEA (from 2 – 10 ml) show progressively higher absorbance at 300 nm, reaching peak values around 330 nm before decreasing to minimum values

near 1100 nm. For example, with 2 ml of TEA, the absorbance at 300 nm starts at 0.11, peaks at 0.61, and drops to 0.04 by 1100 nm. With 10 ml of TEA, absorbance at 300 nm begins at 0.54, peaks at 0.91, and reduces to 0.25 at 1100 nm. Similar trends have been observed in prior studies by [4,14], supporting the consistency of these findings.

Fig. 3 displays the percentage transmittance of MnSe thin films plotted against wavelength. The transmittance generally increases with wavelength but decreases with higher TEA concentrations. For example, a film deposited with 2 ml of TEA has a transmittance of 76.84% at 300 nm, dips to 24.39% at 330 nm, and then rises to 92.17% at 1100 nm. With 10 ml of TEA, the transmittance begins at 28.96% at 300 nm, decreases to 12.53% at 330 nm, and reaches a peak of 55.86% at 1100 nm. Previous findings by [14] show similar transmittance trends, ranging from 67.29% to 90.57% for MnSe films at different pH levels, aligning with this study's results. The valley in the transmittance spectra of the films observed in the UV region corresponds to the MnSe absorption peak. This indicates a significant photon absorption by deposited thin films in this region which correspond to the optical band gap of MnSe. The depth of the valley increases with TEA concentration due to improved crystallinity and reduced surface imperfections, leading to enhanced absorption. This absorption is attributed to electronic transitions between the valence and conduction bands, demonstrating the material's potential for specific optoelectronic applications. The decrease in transmittance with higher TEA concentrations suggests increased porosity and surface imperfections in MnSe thin films as confirmed by SEM and XRD analyses which reveal variations in surface morphology, crystallite size, and structural parameters.

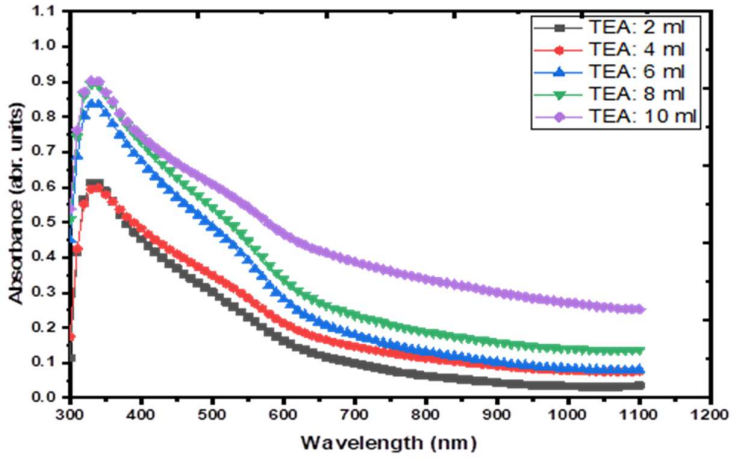

Fig. 2. A plot of Absorbance against wavelength for SILAR deposited Manganese selenide thin films at different volume concentrations of TEA.

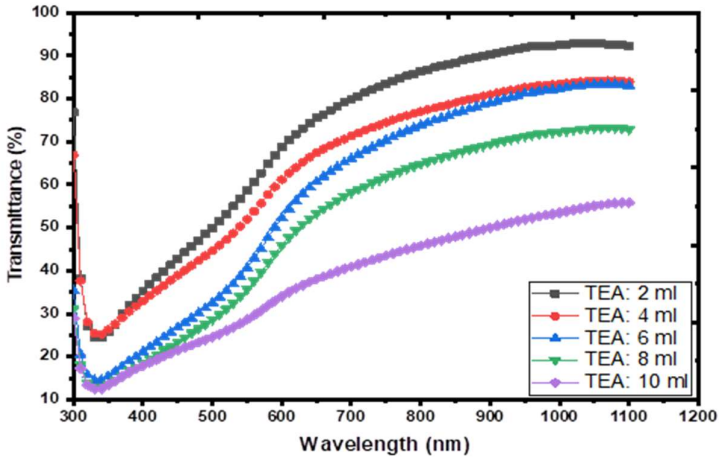

Fig. 3. A plot of the transmittance against wavelength for SILAR deposited Manganese selenide thin films at different volume concentrations of TEA.

Fig. 4 illustrates the reflectance of MnSe thin films across different wavelengths. The films generally show low reflectance in the UV and NIR regions, with peak reflectance reaching 20.35% at specific wavelengths depending on the TEA concentration: 450 nm for 2 ml, 490 nm for 4 ml, 570 nm for 6 ml, 590 nm for 8 ml, and 750 nm for 10 ml of TEA. Films with 8 ml and 10 ml of TEA have negligible reflectance in parts of the UV region, and reflectance values are considered from 360 nm onward. For instance, the film with 2 ml of TEA shows 11.72% reflectance at 300 nm, peaking at 20.35% at 450 nm, and dropping to 4.29% at 1100 nm. In contrast, the film with 10 ml of TEA has an initial reflectance of 1.31% at 360 nm, peaks at 20.35% at 750 nm, and slightly declines to 18.85% at 1100 nm. These low reflectance values suggest that the films are well-suited for anti-reflective coatings in industrial applications.

Fig. 5 presents the refractive index of MnSe thin films across various wavelengths. The films show peak refractive indices of 2.64 at different wavelengths, depending on the TEA concentration: 450 nm for 2 ml, 490 nm for 4 ml, 570 nm for 6 ml, 590 nm for 8 ml, and 750 nm for 10 ml. Films with 8 ml and 10 ml of TEA lack refractive index data in parts of the UV region, with measurements beginning at 360 nm. For example, the film with 2 ml of TEA starts at a refractive index of 2.04 at 300 nm, peaks at 2.64 at 450 nm, and declines to 1.52 by 1100 nm. The film with 10 ml of TEA shows an initial refractive index of 1.19 at 300 nm, rising to 2.64 at 750 nm before decreasing to 2.52 at 1100 nm.

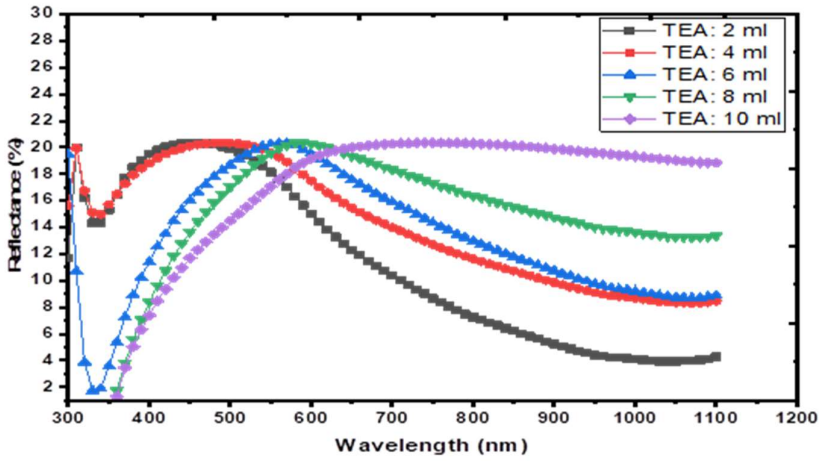

Fig. 4. A plot of the reflectance against wavelength for SILAR deposited Manganese selenide thin films at different volume concentrations of TEA.

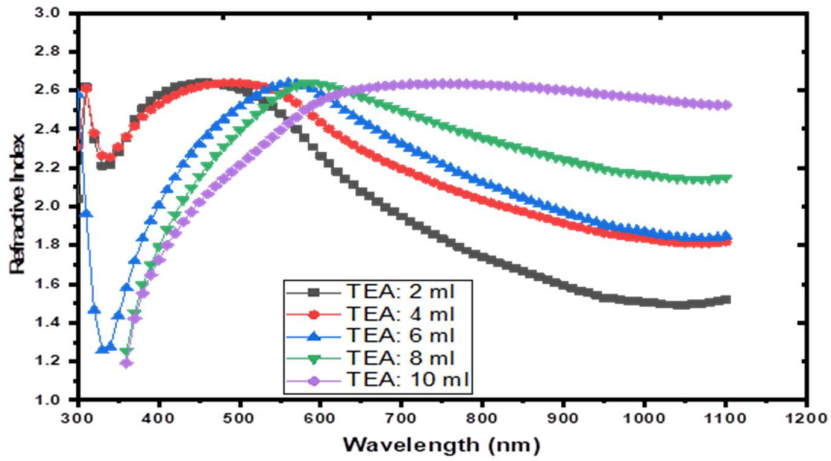

Fig. 5. A plot of the refractive index against wavelength for SILAR deposited Manganese selenide thin films at different volume concentrations of TEA.

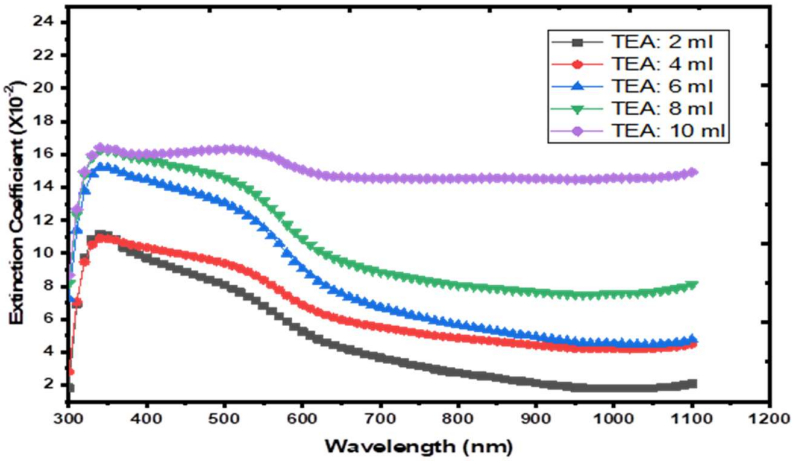

Fig. 6. Plot of extinction coefficient against wavelength for SILAR deposited Manganese selenide thin films at different volume concentration of TEA.

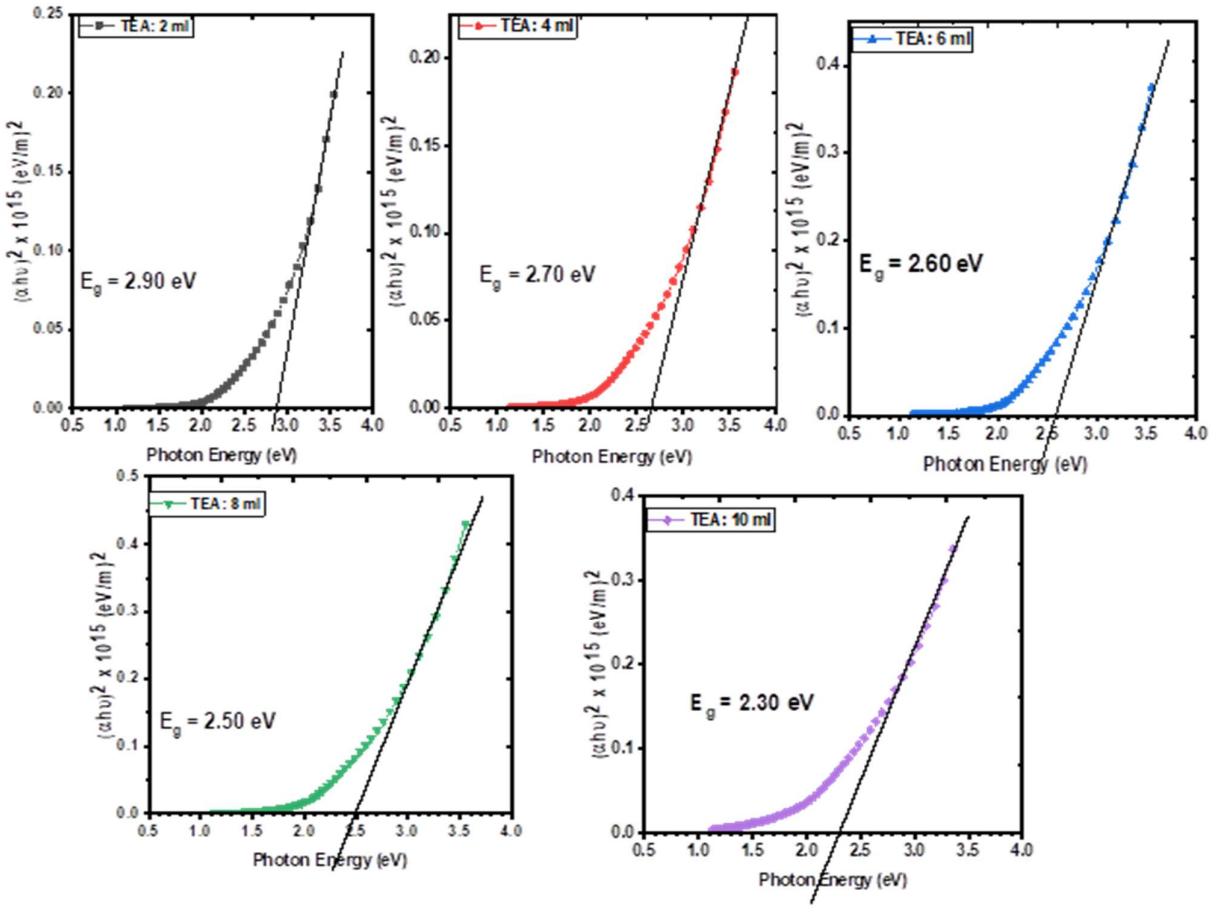

Fig. 7.Plot of (αhν)2 against photon energy for SILAR deposited Manganese selenide thin films at different volume concentration of TEA.

Fig. 6 displays the extinction coefficient of MnSe thin films as a function of wavelength. The extinction coefficient rises within the UV region to a peak at 340 nm, then declines with increasing wavelength, except for the film deposited with 10

ml of TEA, which remains constant across all wavelengths. Additionally, the extinction coefficient increases with higher TEA concentrations. For instance, the film with 2 ml of TEA starts at 1.84×10^{-2} at 300 nm, peaks at 11.15×10^{-2} at 340 nm, and decreases to 2.09×10^{-2} at 1100 nm. Meanwhile, the film with 10 ml of TEA begins at 8.66×10^{-2} at 300 nm, reaches a peak of 16.43×10^{-2} at 340 nm, and then reduces slightly to 14.92×10^{-2} at 1100 nm. The tunable extinction coefficient of MnSe thin films, especially in the UV region, makes them suitable for photovoltaic and photodetector applications, where selective absorption is critical. Additionally, the stable optical properties with higher TEA concentrations offer potential for anti-reflective coatings and optical filtering in optoelectronic devices.

Fig. 7 displays graphs of $(\alpha hv)^2$versus photon energy (hv) for various for TEA concentrations. Direct energy band gap values of the films were determined by extrapolating $(\alpha hv)^2 = 0$ on the photon energy axis. The MnSe thin film with 2 ml of TEA has a band gap of 2.90 eV, decreasing progressively with increasing TEA concentration to 2.30 eV for the film with 10 ml. This indicates that increasing TEA volume concentration effectively reduces the band gap of MnSe films.

Fig. 8 further illustrates the inverse relationship between band gap and TEA concentration. These results are consistent with emission bands of 2.85–3.00 eV obtained by [42] using photoluminescence and align closely with findings by Galyas et al [43]. Reference [4] reported MnSe band gaps between 2.65 eV and 3.80 eV. This demonstrates that TEA concentration can be used to tune the energy band gap in MnSe thin films, making them adaptable for specific optoelectronic applications. Despite the absence of peaks in the visible spectrum, MnSe thin films demonstrate strong UV absorption with a tunable optical band gap between 2.30 eV and 2.90 eV. This positioned the deposited MnSe thin films at the edge of visible light absorption which make them suitable for tandem or multi-junction solar cells, where its ability to capture high-energy photons in the UV region complements materials absorbing lower-energy visible and infrared light.

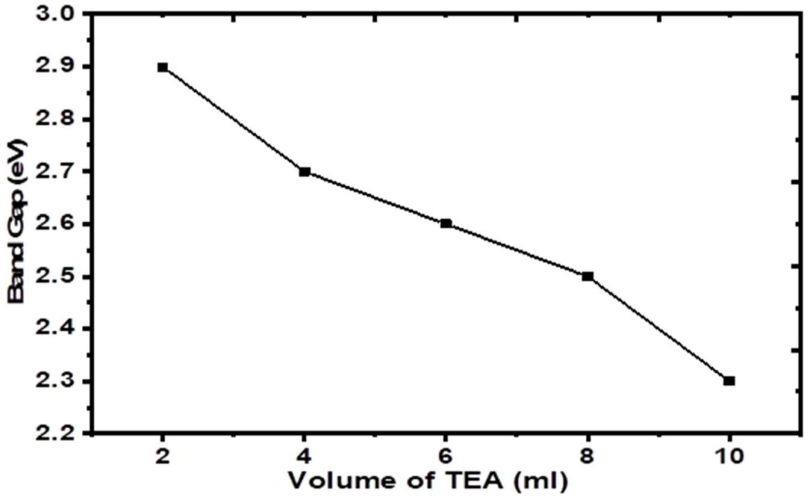

Fig. 8. Plot of energy band gap against volume concentration of TEA for Manganese selenide thin films.

B. Film Thickness Measurement

Fig. 9 presents the film thicknesses obtained using the gravimetric method. The area of the MnSe thin film deposited on the substrates was measured, covering a marked region of 4.5 cm by 2.5 cm (11.25 cm²). The density of bulk MnSe is 5.59 g/cm³, and the change in substrate mass is calculated by weighing the substrates before and after deposition. The film thickness (t) was calculated using (12) [46 – 48].

$$t = \frac{\Delta m}{A\rho} \quad (12)$$

Δm represents the difference in mass of the substrates, A is the area covered by the MnSe thin films, and ρ denotes the bulk density of manganese selenide. Fig. 9 displays the relationship between film thickness and the volume concentration of TEA. The thickness of the deposited films increased from 190.82 nm at 2 ml of TEA to a maximum value of 381.63 nm at 10 ml of TEA as the complexing agent as shown in Table I.

Table I. Thickness parameters using the Gravimetric method

$Vol.Conc._{TEA}$ (ml)	Δm (mg)	A (cm^2)	ρ_{MnSe} $(g/cm3)$	t (nm)
2.00	1.20	11.25	5.59	190.817
4.00	1.40	11.25	5.59	222.620
6.00	1.70	11.25	5.59	270.324
8.00	2.00	11.25	5.59	318.028
10.00	2.40	11.25	5.59	381.634

$Vol.Conc._{TEA}$ is the volume concentration of TEA, Δm is the change in mass, A is the area, ρ_{MnSe} is the density of MnSe and t is the thickness.

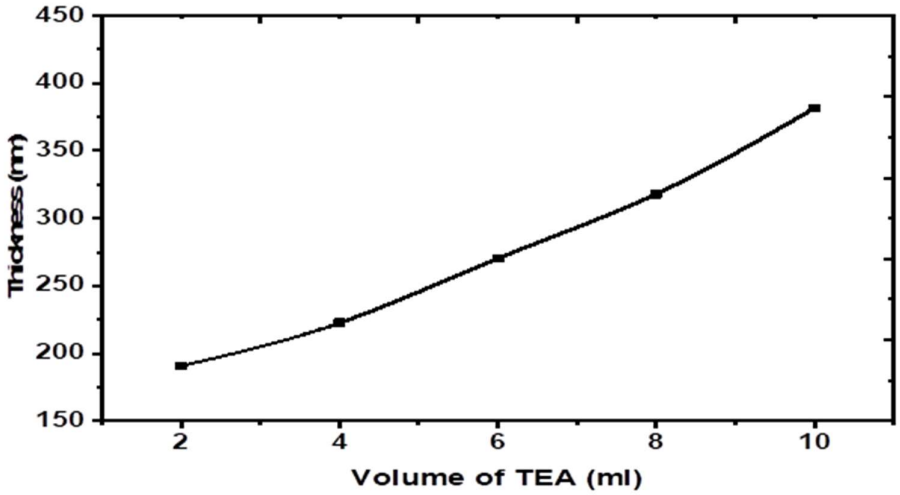

Fig. 9. Plot of thickness (nm) against volume concentration of TEA for Manganese selenide thin films.

C. Electrical Properties of Manganese selenide with volume concentration of TEA

Fig. 10 shows the graph of electrical resistivity and conductivity of SILAR-deposited manganese selenide thin films deposited using different concentrations of TEA. These electrical properties were obtained from current and voltage obtained from four-point probe techniques. The electrical resistivity and conductivity of the films were evaluated using (13) and (14) [40, 49].

The resistivity is given as:

$$\rho = \frac{\pi t}{ln\,2}\left(\frac{V}{I}\right) = 4.523t\left(\frac{V}{I}\right), \quad (13)$$

and electrical conductivity is given as:

$$\sigma = \frac{1}{\rho} \quad (14)$$

where t is the thickness of the films obtained using (12).

Table II shows other electrical properties of the deposited manganese selenide thin films. From Table II, the volume concentration of TEA was found to affect the electrical resistivity and conductivity of SILAR-deposited manganese selenide thin films. Electrical resistivity was found to increase with the increase in the volume concentration of TEA while electrical conductivity was found to decrease with the increase in volume concentration of TEA. This showed that film deposited with 2 ml of TEA was more electrically conductive than manganese selenide deposited with 10 ml of volume concentration of TEA. Electrical resistivity of the manganese selenide thin films ranged from $3.681 \times 10^4\ \Omega cm$ to $9.807 \times 10^4\ \Omega cm$ while the conductivity ranged from 2.717×10^{-5} S/cm and 1.020×10^{-5} S/cm.

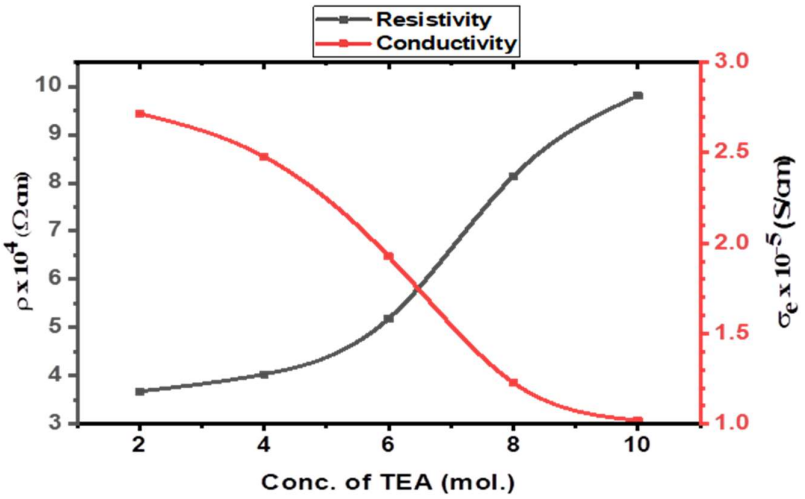

Fig. 10. Electrical properties of SILAR deposited manganese selenide under different volume concentration of TEA.

Table II. Electrical properties of SILAR deposited manganese selenide thin films, deposited under different concentrations of TEA.

Concentrations of TEA $(mol.)$	Voltage (mV)	Current (nA)	Resistance $\times 10^8\ (\Omega)$	Thickness (nm)	sheet resistance $\times 10^9\ (\Omega)$	Resistivity $\times 10^4 (\Omega\ cm)$	Electrical Conductivity $\times 10^{-5}\ (S/cm)$
2	23.420	0.055	4.864	190.817	1.929	3.681	2.717
4	24.010	0.060	3.844	222.620	1.813	4.036	2.478
6	22.892	0.054	4.209	270.324	1.920	5.191	1.926
8	32.191	0.057	6.456	318.028	2.558	8.136	1.229
10	29.498	0.052	4.268	381.634	2.570	9.807	1.020

D. Structural Properties of Manganese selenide with volume concentration of TEA

The structural analysis of SILAR-deposited manganese selenide thin films obtained using Cu–Kα radiation with a wavelength of λ=1.5406 Å reveals a cubic crystal structure, as confirmed by XRD patterns shown in Fig. 11. Prominent peaks corresponding to the (111), (200), (220), (311), and (222) planes are in alignment with the JCPDS file number 00-011-0683. Structural parameters such as crystallite size (D), dislocation density (δ), and microstrain (ε) of the deposited MnSe thin films were determined using (15), (16) and (17) respectively [50], [51 – 53].

$$D = \frac{0.9\,\lambda}{\beta \cos\theta} \quad (15)$$

$$\delta = \frac{1}{D^2} \quad (16)$$

$$\varepsilon = \frac{\beta}{4 \tan\theta} \quad (17)$$

Where β is the full-width half maximum, λ is the wavelength of Cu-Kα1 radiations (1.54056 Å) and θ is the diffraction angle. These structural parameters summarized in Table III, demonstrate clear trends with varying TEA concentrations. The crystallite size increased from 20.097 to 25.091 nm as the volume of TEA increased from 2 to 10 ml, indicating improved crystallinity and grain growth at higher TEA volumes. Simultaneously, the dislocation density decreases from 2.534×10^{15} to 1.654×10^{15} lines/m², while the microstrain reduces from 5.272×10^{-3} to 4.268×10^{-3} reflecting fewer lattice imperfections and reduced lattice distortion. A notable trend is observed in the preferred orientation of the planes, with the (111) and (220) planes showing dominant intensities influenced by TEA concentration. The peak positions show slight shifts (Δ2θ), and the FWHM values decrease at higher TEA concentrations, further indicating improved crystalline quality. Additionally, films deposited with higher TEA volumes exhibit more uniform growth and reduced lattice defects, suggesting enhanced material stability. These findings emphasize the role of TEA as a critical complexing agent, regulating the nucleation and growth processes of the films. The combination of improved crystallite size, reduced strain, and dislocation density makes these films highly promising for optoelectronic and photovoltaic applications, where enhanced crystallinity and structural stability are crucial.

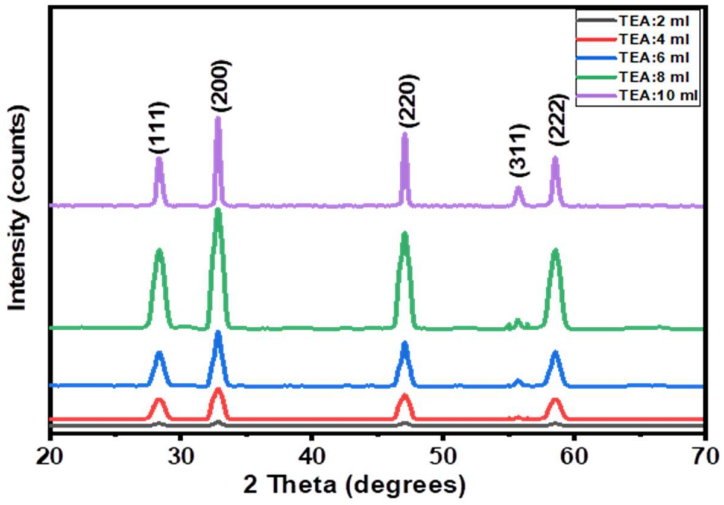

Fig. 11. XRD pattern of SILAR deposited manganese selenide thin films.

Table III. Structural Parameters of manganese selenide thin films at varying volume concentration of TEA

TEA Concentration (ml)	2 θ (◦) Std.	2 θ (◦) Obs.	$\Delta(2\theta)$ (◦)	Observed d-spacing (nm)	FWHM (◦)	D (nm)	δ x 10^{15} (lines/m^2)	ε x 10^{-3}
2	28.291	28.346	-0.055	0.315	0.496	17.268	3.354	8.563
	32.754	32.822	-0.068	0.273	0.416	20.806	2.310	6.159
	47.020	47.056	-0.036	0.193	0.414	21.850	2.095	4.151
	55.807	55.730	0.077	0.165	0.438	21.431	2.177	3.614
	58.479	58.539	-0.060	0.158	0.497	19.132	2.732	3.871
					Average	20.097	2.534	5.272
4	28.291	28.335	-0.044	0.315	0.405	21.128	2.240	7.001
	32.754	32.811	-0.057	0.273	0.426	20.291	2.429	6.317
	47.020	47.043	-0.023	0.193	0.427	21.197	2.226	4.280
	55.807	55.715	0.092	0.165	0.319	29.452	1.153	2.631
	58.479	58.528	-0.049	0.158	0.456	20.873	2.295	3.548
					Average	22.588	2.069	4.755
6	28.291	28.344	-0.05	0.315	0.410	20.876	2.295	7.083
	32.754	32.820	-0.07	0.273	0.473	18.291	2.989	7.006
	47.020	47.053	-0.03	0.193	0.373	24.291	1.695	3.734
	55.807	55.729	0.078	0.165	0.314	29.912	1.118	2.590
	58.479	58.537	-0.06	0.158	0.411	23.157	1.865	3.198
					Average	23.305	1.992	4.722
8	28.291	28.337	-0.05	0.315	0.449	19.055	2.754	7.762
	32.754	32.813	-0.06	0.273	0.419	20.622	2.351	6.216
	47.020	47.044	-0.02	0.193	0.420	21.546	2.154	4.210
	55.807	55.719	0.088	0.165	0.238	39.516	0.640	1.961
	58.479	58.529	-0.05	0.158	0.450	21.147	2.236	3.502
					Average	24.377	2.027	4.730
10	28.291	28.356	-0.07	0.314	0.413	20.723	2.329	7.133
	32.754	32.828	-0.07	0.273	0.333	25.942	1.486	4.939
	47.020	47.071	-0.05	0.193	0.323	27.997	1.276	3.238
	55.807	55.737	0.07	0.165	0.407	23.066	1.880	3.358
	58.479	58.550	-0.07	0.158	0.343	27.728	1.301	2.670
					Average	25.091	1.654	4.268

Fig. 12 shows the SEM images of manganese selenide thin films deposited using the SILAR method with varying volumes of triethanolamine (TEA). These micrographs revealed significant morphological differences in the deposited thin film. The film with 2 ml of TEA shows a relatively smooth surface with scattered small clusters, indicating localized nucleation and incomplete coverage. Increasing the TEA volume to 4 ml results in a granular texture with more uniformly distributed clusters, enhancing nucleation sites but still displaying some porosity. At 6 ml, the film exhibits improved surface coverage with prominent grain-like structures and some small cracks, suggesting stress during growth. The 8 ml sample features elongated, rod-like formations, indicating a shift to a more organized growth mechanism due to increased TEA complexation effects, which may enhance functional properties. In contrast, the 10 ml film shows a drastic change with larger, flake-like structures, leading to a less uniform surface and increased porosity. Overall, while the 6 ml TEA volume seems to provide a balanced combination of uniformity and coverage, higher volumes may result in larger structures and defects, which could impact the films' properties negatively. The findings highlight the importance of optimizing TEA volume to tailor the morphology of MnSe films for specific applications.

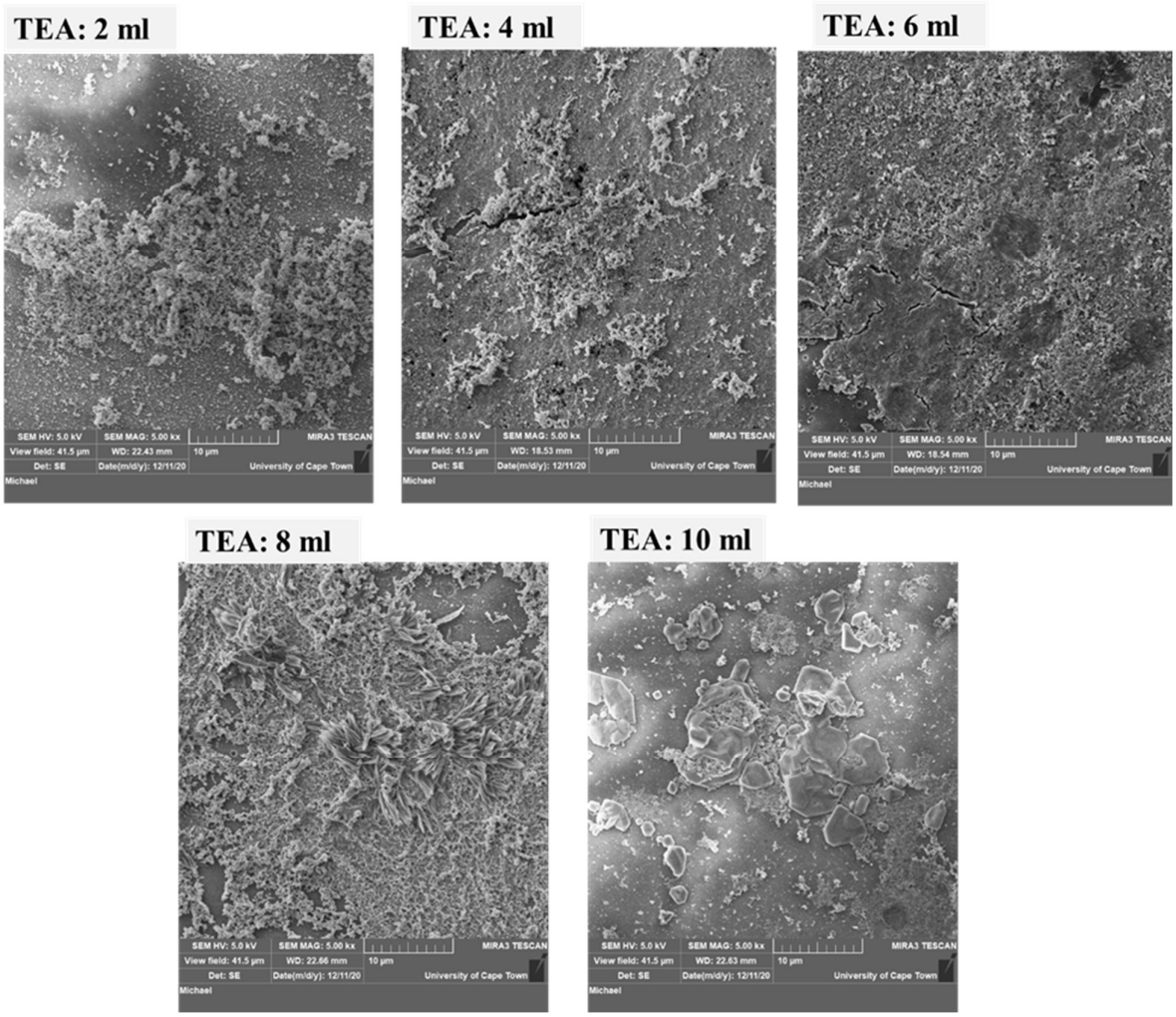

Fig. 12. SEM images of manganese selenide thin films.

IV. CONCLUSION

This study successfully synthesized manganese selenide (MnSe) thin films using the Successive Ionic Layer Adsorption and Reaction (SILAR) method while varying the volume of triethanolamine (TEA) as a complexing agent. The research aimed to evaluate the potential of MnSe as an absorber layer for thin-film solar cells, focusing on its optical, electrical, structural and morphological properties. The results demonstrated that variation in TEA volume significantly influences the material's properties. The energy band gap, a critical parameter for photovoltaic applications, decreased from 2.90 eV to 2.30 eV as TEA volume increased from 2 ml to 10 ml, indicating improved absorption in the visible light spectrum. Film thickness varied from 190.82 nm to 381.63 nm, reflecting a direct relationship with TEA concentration. Structurally, the MnSe films crystallized in the cubic phase with improved crystallinity and reduced defects at higher TEA volumes, as evidenced by a crystallite size increase from 20.10 nm to 25.09 nm and decreased dislocation density and microstrain. Morphological analysis revealed uniform grain-like structures at moderate TEA concentrations, which are optimal for photovoltaic performance. The electrical properties highlighted a trade-off between resistivity and conductivity. Films deposited with lower TEA volumes exhibited higher electrical conductivity (2.72×10^{-5} S/cm at 2 ml) compared to those with higher TEA volumes (1.02×10^{-5} S/cm at 10 ml), aligning with reduced grain boundary resistance. These findings confirm the suitability of MnSe thin films for absorber layers in solar cells, particularly where tunable optical and electrical properties are desired. The ability to control these properties by varying TEA concentration enhances the material's versatility for applications beyond photovoltaics, including optoelectronic and photodetector devices.

ACKNOWLEDGEMENT

This research was fully funded by Institutional Based Research (IBR) of the Tertiary Education Trust Fund (TETFund) of Nigeria through Delta State Polytechnic,

Ogwashi-Uku, Delta State, Nigeria.

CONFLICT OF INTEREST

The authors declare that they have no known competing financial or other interests that could have influenced this study.

DATA AVAILABILITY

The authors declare that the data supporting the findings of this study are available on request.

AUTHOR CONTRIBUTIONS

All authors contributed to the study's conception and design. Asielue O Kingsley, Opene, J Nkechi and Okoli N Livinus performed material preparation, experiments, data collection and analysis. All the authors wrote the first draft of the manuscript. Asielue O Kingsley and Okoli N Livinus participated in the discussion and gave some valuable suggestions. Opene J Nkechi and Okoli N Livinus revised the manuscript before submission. All authors read and approved the final version of the manuscript.

References

[1] V. Jevtovic, A. U. Khan, Z. M. Almarhoon, K. Tahir, S. Latif, F. Abdulaziz, K. Albalawi, M. E. A. Zaki and V. Rakic. “Synthesis of MnSe-Based GO Composites as Effective Photocatalyst for Environmental Remediations:. Nanomat., vol. 13, no. 667, 2023. https://doi.org/10.3390/nano13040667

[2] T. Mahalingam, S. Thanikaikarasan, V. Dhanasekaran, A. Kathalingam, and S. Velumani. Preparation and characterization of MnSe thin films. Mat. Sci. & Eng.: B, vol. 174, no. 3, pp. 257–262, 2010. https://doi.org/10.1016/j.mseb.2010.03.026

[3] Q. Peng, Y. Dong, Z. Deng, H. Kou, S. Gao and Y. Li. “Selective synthesis and magnetic properties of α-MnSe and $MnSe_2$ uniform microcrystals”. The J. of Phy. Chem. B, vol. 106, no. 35, pp. 9261–9265, 2002. https://doi.org/10.1021/jp020635f

[4] I. T. Sines, R. Misra, P. Schiffer and R. E. Schaak. “Colloidal synthesis of non-equilibrium wurtzite-type MnSe”. Angewandte Chemie Int. Ed., vol. 49, no. 26, pp. 4742–4744, 2010. https://doi.org/10.1002/anie.201001213

[5] P. Tomasini, A. Haidoux, J. C. Tedenac and M. Maurin. “Methylpentacarbonylmanganese as organometallic precursor for the epitaxial growth of manganese selenide heterostructures”. J. of Cryst. Growth, vol. 193, no. 1-2, pp.572-576, 1998. https://doi.org/10.1016/S0022-0248(98)00607-1

[6] X. Liu, J. Ma, P. Peng, and W. Zheng, "Hydrothermal synthesis of cubic $MnSe_2$ and octahedral α-MnSe microcrystals," Journal of Crystal Growth, vol. 311, no. 6, pp. 1359–1363, 2009. https://doi.org/10.1016/j.jcrysgro.2008.12.054

[7] M.-Z. Xue and Z.-W. Fu, "Investigation of MnSe-based composites for energy applications," Solid State Ionics, vol. 178, no. 3-4, pp. 273–279, 2007. https://doi.org/10.1016/j.ssi.2006.12.020

[8] M. Aapro, M. N. Huda, K. Jeyakumar, K. Shawulienu, S. C. Ganguli, H. Gonzalez Herrero, X. Huang, P. Liljeroth, and H.-P. Komsa, "Synthesis and properties of monolayer MnSe with unusual atomic structure and antiferromagnetic ordering," *ACS Nano*, vol. 15, no. 8, pp. 13794–13802, 2021. https://doi.org/10.1021/acsnano.1c05532

[9] M.-Z. Xue and Z.-W. Fu, "Manganese selenide thin films as anode material for lithium-ion batteries," *Solid State Ionics*, vol. 178, no. 3-4, pp. 273–279, 2007. https://doi.org/10.1016/j.ssi.2006.12.020

[10] D. J. O’Hara, T. Zhu, A. H. Trout, A. S. Ahmed, Y. K. Luo, C. H. Lee, M. R. Brenner, S. Rajan, J. A. Gupta, D. W. McComb, and R. K. Kawakami, "Room temperature intrinsic ferromagnetism in epitaxial manganese selenide films in the monolayer limit," *Nano Letters*, vol. 18, no. 5, pp. 3125–3131, 2018. https://doi.org/10.1021/acs.nanolett.8b00683

[11] W.-p. Li, C.-h. Li, S. Ma, Z.-m. Xie, and S.-t. Zhang, "Study on characterization and electrodeposition of MnSe/Ti thin films," *Journal of Functional Materials*, vol. 44, no. 11, pp. 1635–1637, 2013.

[12] X. Yang, B. Zhou, C. Liu, and X. et al., "Unravelling a solution-based formation of single-crystalline kinked wurtzite nanowires: The case of MnSe," *Nano Research*, vol. 10, no. 8, pp. 2311–2320, 2017. https://doi.org/10.1007/s12274-017-1424-7

[13] J. Zhang, F. Zhang, X. Zhao, X. Wang, L. Yin, C. Liang, M. Wang, Y. Li, J. Liu, Q. Wu, and R. Che, "Uniform wurtzite MnSe nanocrystals with surface-dependent magnetic behavior," *Nano Research*, vol. 6, no. 4, pp. 275–285, 2013. https://doi.org/10.1007/s12274-013-0305-y

[14] İ. A. Kariper, "A new route to synthesize MnSe thin films by chemical bath deposition method," *Materials Research*, vol. 21, no. 2, e20170215, 2018. https://doi.org/10.1590/1980-5373-MR-2017-0215

[15] A. Le Donne, V. Trifiletti, and S. Binetti, "New earth-abundant thin film solar cells based on chalcogenides," *Frontiers in Chemistry*, vol. 7, p. 297, 2019. https://doi.org/10.3389/fchem.2019.00297

[16] B. R. Sankapal, R. S. Mane, and C. D. Lokhande, "Successive ionic layer adsorption and reaction (SILAR) method for the deposition of large area (~10 cm^2) tin disulfide (SnS_2) thin films," *Materials Research Bulletin*, vol. 35, no. 12, pp. 2027–2035, 2000. https://doi.org/10.1016/S0025-5408(00)00347-9

[17] H. Soonmin, "Recent advances in the growth and characterizations of SILAR-deposited thin films,"

Applied Sciences, vol. 12, no. 16, p. 8184, 2022. https://doi.org/10.3390/app12168184

[18] M. A. Patwary, "Thin films processed by SILAR method," *IntechOpen*, 2023.. https://doi.org/10.5772/intechopen.106476

[19] H. Soonmin and N. Shiong, "Effect of pH on the synthesis of cobalt selenide films by SILAR method," *Oriental Journal of Chemistry*, vol. 37, pp. 791–796, 2021. http://dx.doi.org/10.13005/ojc/370404

[20] N. J. Egwunyenga, O. V. C. Okoli, N. L. Okoli, and I. E. Nwankwo, "Effect of SILAR cycles on the thickness, structural, and optical properties of cobalt selenide thin films," *International Research Journal of Multidisciplinary Technovation*, vol. 3, no. 4, pp. 1–9, 2021. https://doi.org/10.34256/irjmt2141

[21] A. Astam, Y. Akaltun, and M. Yıldırım, "Conversion of SILAR deposited Cu_3Se_2 thin films to $Cu_{2-x}Se$ by annealing," *Materials Letters*, vol. 166, pp. 9–11, 2016. https://doi.org/10.1016/j.matlet.2015.12.070

[22] A. Ivanauskas, R. Ivanauskas, and I. Ancutiene, "Effect of In-incorporation and annealing on Cu_xSe thin films," *Materials*, vol. 14, no. 14, p. 3810, 2021. https://doi.org/10.3390/ma14143810

[23] P. M. Geethanjali, K. Deepa, and T. L. Remadevi, "Effect of number of cycles on SILAR deposited ZnSe thin films," *AIP Conference Proceedings*, vol. 2352, no. 1, p. 020011, 2021. https://doi.org/10.1063/5.0052381

[24] R. B. Kale and C. D. Lokhande, "Room temperature deposition of ZnSe thin films by successive ionic layer adsorption and reaction (SILAR) method," *Materials Research Bulletin*, vol. 39, no. 12, pp. 1829–1839, 2004. https://doi.org/10.1016/j.materresbull.2004.06.027

[25] S. D. Khot, D. B. Malavekar, R. P. Nikam, S. B. Ubale, P. P. Bagwade, D. J. Patil, V. C. Lokhande, and C. D. Lokhande, "SILAR synthesized dysprosium selenide (Dy_2Se_3) thin films for hybrid electrochemical capacitors," *Synthetic Metals*, vol. 287, p. 117075, 2022. https://doi.org/10.1016/j.synthmet.2022.117075

[26] H. Ertap, M. Yuksek, and M. Mevlut, "Structural and optical properties of indium selenide (InSe) thin films deposited on glass and GaSe single crystal substrates by SILAR method," *Cumhuriyet Science Journal*, vol. 40, pp. 602–611, 2019. https://doi.org/10.17776/csj.519415

[27] K. B. Chaudhari, N. M. Gosavi, N. G. Deshpande, and S. R. Gosavi, "Chemical synthesis and characterization of CdSe thin films deposited by SILAR technique for optoelectronic applications," *Journal of Science: Advanced Materials and Devices*, vol. 1, no. 4, pp. 476–481, 2016.

[28] C. I. Elekalachi, I. A. Ezenwa, A. N. Okereke, and N. L. Okoli, "Influence of annealing temperature on the properties of SILAR deposited CdSe/ZnSe superlattice thin films for optoelectronic applications," *Nanoarchitectonics*, vol. 4, no. 1, pp. 26–44, 2022. https://doi.org/10.37256/nat.4120231650

[29] M. Xu, W. Zhong, J. Yu, W. Zang, C. Au, Z. Yang, L. Lv, and Y. Du, "Exchange-bias-like behavior from disordered surface spins in $Li_4Mn_5O_{12}$ nanosticks," *The Journal of Physical Chemistry C*, vol. 114, no. 39, pp. 16143–16147, 2010. https://doi.org/10.1021/jp101746f

[30] Y. Zhao, R. Yang, K. Yang, J. Dou, X. Yang, J. Guo, G. Zhou, and X. Xu, "Anomalous magnetic property and broadband photodetection in ultrathin non-layered manganese selenide semiconductor," *Nano Research*, vol. 17, no. 9, pp. 8578–8584, 2024. https://doi.org/10.1007/s12274-024-6855-3

[31] N. J. Egwunyenga, V. C. Onuabuchi, N. L. Okoli, and I. E. Nwankwo, "Effect of SILAR cycles on the thickness, structural, optical properties of cobalt selenide thin films," *International Research Journal of Multidisciplinary Technovation*, vol. 3, no. 4, pp. 1–9, 2021. https://doi.org/10.34256/irjmt2141.

[32] M. Sozanskyi, V. Stadnik, P. Shapoval, I. Yatchyshyn, R. Guminilovych, and S. Shapoval, "Optimization of synthesis conditions of mercury selenide thin films," *Chemistry & Chemical Technology*, vol. 14, no. 3, pp. 290–296, 2020. https://doi.org/10.23939/chcht14.03.290

[33] S. Samanta, M. S. Shinde, and R. S. Patil, "Synthesis and characterization of cadmium selenide nanocrystalline thin films prepared using a novel chemical approach," *Journal of Nano and Advanced Materials*, vol. 4, no. 2, pp. 53–57, 2016. http://dx.doi.org/10.18576/jnam/040202

[34] H. M. Pathan, B. M. Palve, S. S., E. R. Jadkar, and O.-S. Joo, "Nanocrystalline copper selenide formation by direct reaction between Cu-ions and selenosulfate," *ES Materials & Manufacturing*, vol. 10, pp. 39–44, 2020. http://dx.doi.org/10.30919/esmm5f905

[35] S. R. Devi, P. J. Saikia, and M. A. Hussain, "Studies on optical and electrical properties of PVA-capped nanocrystalline CdSe thin film prepared by chemical bath deposition method," *Chalcogenide Letters*, vol. 19, no. 12, pp. 901–908, 2022.

[36] K. Ahmad, Z. Almutairi, S. M. Ali, R. Almuzaiqer, C. Wan, and A. Sayeed, "Synthesis, characterization and power factor estimation of SnSe thin film for energy harvesting applications," *Processes*, vol. 12, no. 4, p. 665, 2024. https://doi.org/10.3390/pr12040665

[37] Raval, A. V., Shaikh, I. A., Doshi, Y. N., Shastri, N. M., Saini, L. K., & Shah, D. V. (2022). Nano-crystalline tin selenide thin films: Synthesis and characterization. *Materials Today Chemistry, 24*, 100762. https://doi.org/10.1016/j.mtchem.2022.100762

[38] C. B. Muomeliri, A. J. Ekpunobi, D. N. Okoli, C. Okafor, J. D. Mimi, O. E. Odikpo, O. Anusiobi, A.

Nwaodo, A. Azubogu, L. Ozobialu, E. O., C. O. Chiamaka, I. Chibuogwu, A. N. Nwori, and N. L. Okoli, "Influence of Ti doping on the optical and structural properties of ZnTiO thin films deposited by electrodeposition technique," *Journal of Materials Science Research and Reviews*, vol. 7, no. 4, pp. 493–506, 2024.

[39] C. J. Nkamuo, N. L. Okoli, F. N. Nzekwe, and N. J. Egwunyenga, "Tuning the properties of manganese-doped zinc oxide nanostructured thin films deposited by SILAR approach," *Chemistry of Inorganic Materials*, vol. 2, p. 100038, 2024. https://doi.org/10.1016/j.cinorg.2024.100038

[40] N. L. Okoli, L. N. Ezenwaka, N. A. Okereke, I. A. Ezenwa, and N. A. Nwori, "Investigation of optical, structural, morphological and electrical properties of electrodeposited cobalt doped copper selenide (Cu(1-x)CoxSe) thin films," *Trends in Sci.s*, vol. 19, no. 16, p. 5686, 2022. https://doi.org/10.48048/tis.2022.5686

[41] N. Khan, A. Javed, M. Bashir, and S. Bashir, "Role of triethanolamine complexing agent in chemical bath deposition of tin sulfide thin films: Microstructural and optical properties," *Results in Optics*, vol. 14, p. 100610, 2024. https://doi.org/10.1016/j.rio.2024.100610

[42] H. J. Chun, J. Y. Lee, D. S. Kim, S. W. Yoon, J. H. Kang, and J. Park, "Morphology-tuned growth of α-MnSe one-dimensional nanostructures," *Journal of Phy.al Chem. C*, vol. 111, no. 2, pp. 519–525, 2007. https://doi.org/10.1021/jp0658187

[43] A. I. Galyas, O. F. Demidenko, and G. I. Makovetskii, "Transmission spectra of films of $Mn_{1-x}Fe_xSe$ solid solutions," *Journal of Applied Spectroscopy*, vol. 74, no. 1, pp. 152–155, 2007. https://doi.org/10.1007/s10812-007-0023-x

[44] L. P. Joshi, L. Risal, and S. P. Shrestha, "Effects of concentration of triethanolamine and annealing temperature on band gap of thin film of tin sulfide prepared by chemical bath deposition method," *J. of Nepal Phy. Soc.*, vol. 3, no. 1, pp. 1–5, 2016. https://doi.org/10.3126/jnphyssoc.v3i1.14436

[45] K. Manikandan, P. Mani, C. S. Dilip, S. Valli, P. F. H. Inbaraj, and J. J. Prince, "Effect of complexing agent TEA: The structural, morphological, topographical, and optical properties of FexSx nano thin films deposited by SILAR technique," *Applied Surf. Sci.*, vol. 288, pp. 76–82, 2014. https://doi.org/10.1016/j.apsusc.2013.09.109

[46] S. A. Hameed, Z. Saadmahdi, A. N. Jasim, A. F. Taha, and A. A. Habeeb, "Effect of thickness on structural and optical properties of CdO thin films prepared by chemical spray pyrolysis method," *NeuroQuantology*, vol. 18, no. 4, pp. 20–26, 2020. https://doi.org/10.14704/nq.2020.18.4.NQ20156

[47] H. Güney and M. E. Ertargın, "Effective annealing of ZnO thin films grown by three different SILAR processes," *Eastern Anatolian Journal of Science*, vol. 1, no. 1, pp. 20–24, 2015.

[48] F. Gode and S. Unlu, "Nickel doping effect on the structural and optical properties of indium sulfide thin films by SILAR," *Open Chemistry*, vol. 16, pp. 757–762, 2018. https://doi.org/10.1515/chem-2018-0089

[49] I. A. Ezenwa, N. A. Okereke, and N. L. Okoli, "Electrical properties of copper selenide thin film," *IPASJ Int. J. of Elect. Eng. (IIJEE)*, vol. 1, no. 6, pp. 1–6, 2013.

[50] C. Elekalachi, . I. A. Ezenwa, N. A. Okereke, N. L. Okoli, and A. N. Nwori, "Thermal Annealing Impact on the Properties of CdSe/PbSe Superlattice Thin Films: CdSe/PbSe Superlattice Thin Films", *Mater. Devices*, vol. 8, Nov. 2024. https://doi.org/10.23647/ca.md20240211

[51] S. O. Aisida, N. Madubuonu, M. H. Alnasir, I. Ahmad, S. Botha, M. Maaza, and F. I. Ezema, "Biogenic synthesis of iron oxide nanorods using *Moringa oleifera* leaf extract for antibacterial applications," *App. Nanosci.*, vol. 10, no. 1, pp. 305–315, Jan. 2020. https://doi.org/10.1007/s13204-019-01099-x

[52] A. Alshoaibi, P. O. Ike, C. Awada, E. O. Echeweozo, S. Islam, and F. I. Ezema, "Gadolinium doped lithium aluminum borate $[Li_3Al_3(BO_3)_4:Gd]$ materials synthesized and characterized for its structural, optical and thermoluminescence properties for use in dosimetric application," *Rad. Phy. & Chem.*, vol. 229, p. 112445, Apr. 2025. https://doi.org/10.1016/j.radphyschem.2024.112445

[53] E. O. Okechukwu, I. L. Ikhioya, and A. J. Ekpunobi, "Investigating the influence of precursor temperature on the bandgap energy, structural, and morphological features of Ti-doped barium sulphide material for photovoltaic application," *PHYSICSAccess,* vol. 4, no. 1, pp. 64, 2024. https://doi.org/10.47514/phyaccess.2024.4.1.008